Atmos. Meas. Tech. Discuss., 3, 1133–1162, 2010
www.atmos-meas-tech-discuss.net/3/1133/2010/

Atmospheric
Measurement
Techniques
Discussions

Chemical ionization mass spectrometer (CIMS) for ambient measurements of ammonia

D. R. Benson[1], **M. Al-Refai**[2], **and S.-H. Lee**[1]

[1]Kent State University, Department of Chemistry, Kent, Ohio, USA
[2]Kent State University, Department of Computer Sciences, Kent, Ohio, USA

Received: 23 February 2010 – Accepted: 3 March 2010 – Published: 24 March 2010

Correspondence to: S.-H. Lee (slee19@kent.edu)

Published by Copernicus Publications on behalf of the European Geosciences Union.

Abstract

This study describes a chemical ionization mass spectrometer (CIMS) for fast response, in-situ measurements for gas phase ammonia. Protonated ethanol ions were used as the ion-molecule reaction reagent. The CIMS sensitivity was estimated to be between 4–25 Hz/pptv with 30% uncertainty. The instrument background was below 1 ppbv and at lowest was 300 pptv. The uncertainty associated with the instrumental background was less than 30 pptv under the optimized experimental conditions. The time response was less than 30 s, and the detection limit was approximately 60 pptv. This CIMS was used to measure the ambient NH_3 in Kent, Ohio, for several weeks throughout three seasons. The measured ammonia mixing ratios were usually at the sub-ppbv level, and higher during the spring (200±120 pptv) than in the winter (60±75 pptv) and fall (150±80 pptv).

1 Introduction

Ammonia (NH_3) is prevalent in the atmosphere and serves as the principal base gas phase species. NH_3 can control the acidity of the atmospheric aerosols and in turn, change the chemical composition, reactivity, hygroscopicity, and optical properties of aerosol particles. Atmospheric observations (Weber et al., 1998; McMurry et al., 2005) and aerosol microphysical modeling simulations (Stanier et al., 2004; Gaydos et al., 2005; Lucas and Akimoto, 2006; Jung et al., 2008) have suggested that NH_3 can be important for atmospheric nucleation on the global and regional scale. Chemical analysis of aerosol composition also showed that newly formed atmospheric aerosol particles indeed contain ammonium and sulfate along with other components (Smith et al., 2005). Laboratory nucleation observations (Ball et al., 1999; Benson et al., 2009) further demonstrated that NH_3 can enhance sulfuric acid and water homogeneous nucleation (Merikanto et al., 2007).

Sources of NH_3 stem mostly from anthropogenic emissions such as livestock excrement, biomass burning, fertilizer application, and automobile emissions (Schlesinger and Hartley, 1992; Dentener and Crutzen, 1994; Fraser and Cass, 1998; Kean et al., 2000; Moeckli et al., 2004). Tropospheric NH_3 mixing ratios range from several pptv up to several hundreds ppbv and sometimes even up to several hundreds ppmv levels (Gilliland et al., 2003; Huai et al., 2003; Herndon et al., 2005; Li et al., 2006; Nowak et al., 2007), depending on the proximity to emission sources, altitude, and acidity of aerosol particles present in the atmosphere. Since even sub ppbv levels of NH_3 may be responsible for nucleation events observed in certain atmospheric conditions (Gaydos et al., 2005; Jung et al., 2008) and because nucleation takes place rapidly, it is important to have a technique capable of measuring low concentrations of NH_3 with a fast time response, so that we can identify the role of ammonia in aerosol nucleation from in-situ real-time observations.

Reliable measurements of NH_3 are difficult, because of different forms present in the atmosphere, for example, gaseous NH_3, particulate $(NH_4)_2SO_4$, NH_4HSO_4, NH_4NO_3, and liquid NH_4OH. NH_3 is a also very sticky molecule, so when even extremely clean air is introduced into the sampling inlet, there are always substantial NH_3 signals (background signals) due to adsorption and desorption of NH_3 on various surfaces; and, the instrument detection limit is ultimately dependent on background signals. The instrument time response is also affected by adsorption and desorption of NH_3. Uncertainty resulted from background and calibration measurements are another important issue to address for accurate detection of NH_3.

Different measurement techniques have been developed, including citric acid denuder (Ferm et al., 1988), molybdenum-oxide converter-difference (Langford et al., 1989), tungsten oxide denuder (Lebel et al., 1985), photofragmentation/laser induced fluorescence (van Dijk et al., 1989), and filterpack/colorimetry (Quinn and Bates, 1989). Amongst, the citric acid denuder technique is the most commonly used method, as this technique has a high accuracy (within 10%), a simple system, a low cost as well as a low detection limit (25 pptv). For these reasons, it has also served as the standard method to which the other techniques are judged, but the time resolution is poor (e.g. 2 h). (Schwab et al., 2007) also discussed about several different methods of ammonia measurements, such as ion mobility spectrometer, tunable diode laser adsorption spectrometer, long path adsorbtion photometer, wet effluent diffusion denuder and chemiluminescence analyzer. Most of these instruments have a low detection limit (<200 ppt) with 1 min integration time. Most of these measurement values were within 25% of the standard calibration value. However, some of the instruments also showed a slow response time to calibration and ambient measurements based on measurement histories.

Recently, chemical ionization mass spectrometers (CIMS) have been used for fast time resolution detection for NH_3 (Nowak et al., 2006; Norman et al., 2007; Nowak et al., 2007). These instruments were used in both ground-based (Nowak et al., 2006; Norman et al., 2007) and aircraft studies (Nowak et al., 2007). A summary of NH_3-CIMS from these pre-existing techniques is given in Table 1 and will be discussed in detail in Sect. 5 in comparison with our CIMS. The most significant advantage of CIMS, compared to other techniques, is fast time response (<1 min). On the other hand, the lowest achievable background in CIMS is only about a few hundred pptv and the stability of the background can be poor.

In this study, we describe our CIMS instrument for in-situ NH_3 detection. Since the key technical issues for NH_3 detection are the instrument background, calibration and time response, our focus is here to address these key technical issues. We will also discuss atmospheric observation results of NH_3 taken in Kent, Ohio (a relatively less polluted US Midwestern town), including its seasonal variation.

2 Instrument

The NH_3-CIMS system consists of the following three parts: (i) a sampling inlet to perform ambient, background and calibration measurements, (ii) the CIMS flow reactor where ion-molecule reactions occur, and (iii) the vacuum regions of the mass spectrometer including a collision dissociation chamber (CDC), an octopole ion guide, a quadrupole mass filter and a channeltron detector (Fig. 1a).

The third part of the mass spectrometer (vacuum region) is similar to that of the GaTech NH_3-CIMS (Nowak et al., 2006) and the H_2SO_4-CIMS described elsewhere (Eisele and Tanner, 1993; Benson et al., 2008; Young et al., 2008). Below, we only describe the inlet and flow tube regions (Sects. 2.2 and 2.3). The CDC and octopole ion guide dramatically improve the instrument sensitivity and cleanness of the ion mass spectra (Fig. 1a) (Sect. 2.3). This is one of the major advantages of our CIMS, along with NOAA and GaTech NH_3-CIMS instruments (Nowak et al., 2006, 2007), compared to some of the other CIMS instruments currently used for atmospheric observations of various trace gases.

We also note that our CIMS measures only gas phase NH_3, as opposed to ammonium (NH_4^-) present in solid or liquid aerosol phases. This is because CIMS techniques are based on gas phase ion-molecule reactions (e.g. Reaction R1 in Sect. 2.3). To detect aerosol phase NH_4^+, thermal desorption or laser ablation is needed to vaporize these ammonium components into the gas phase for further mass spectrometer analysis; but this is not the case for our CIMS.

2.1 Measurement site

The ambient measurements were performed from the top floor of Williams Hall (15 m above the ground level) at Kent State University in Kent, Ohio (41.15° N, 81.36° W), for several weeks covering three seasons starting from winter of 2008 to fall of 2009. Kent is a small college town with a population of about 30 000 located in Northeastern Ohio. Kent is relatively rural itself, but is also surrounded by three urban cities, about 60 km southeast of Cleveland, about 30 km east of Akron, and about 120 miles west from Youngstown. The weather in Ohio is humid especially in summer. Northeastern Ohio is also known for its haze and gray colored sky in winter. Northeastern Ohio has rich vegetation with numerous large forests. Ohio is also one of the states that currently suffer from air pollution problems, failing to attain the National Air Quality

Standards (NAAQS) for ozone and $PM_{2.5}$ (particulate matter smaller than 2.5 µm) (http://www.epa.gov/air/airtrends/pm.html).

2.2 Inlet

Our inlet system used for background, ambient and calibration measurements was based on the GaTech NH_3-CIMS instrument (Nowak et al., 2006) with some differences discussed here in detail. Special care was taken to make the entire system as short and simple as possible to reduce the residence time of the sampling gases in the inlet tubing. For calibration, we have tried to minimize the dead volume of the tubing to shorten the instrument response time. Only PFA and FEP Teflon materials were used in the inlet system, as stainless steel or other metal materials can easily uptake ammonia on their surfaces (Yokelson et al., 2003b; Nowak et al., 2006, 2007).

Figure 1 illustrates one of the setups used for ambient measurements during fall 2009. With this configuration, we observed the lowest background signals and fastest instrument time response. The outer portion of the inlet consisted of a 65 cm, 1/4 inch (1 inch=2.54 cm) OD fluorinated ethylene-propylene (FEP) tube (the depth of the wall of Williams Hall is 50 cm) that stuck out a 1/2 inch hole in our laboratory wall. This tube was connected to a PFA tee with the other ports connected to a 3-way PFA valve and NH_3 scrubber housing via 1/4 inch OD FEP tubing. For the ambient measurement mode, air traveled through the tee and through 15 cm of the FEP tubing into the 3-way valve (ambient mode flow is shown by orange arrow in Fig. 1). When performing background measurements, ambient air entered the PFA tee and traveled through 30 cm of the FEP tubing into the scrubber housing (stainless steel, 3.5 cm ID, 15 cm long) out the exit of the housing through 40 cm of the FEP tubing and into the 3-way valve (background mode flows are illustrated in blue arrows in Fig. 1). The scrubber housing contained silicon phosphates (Perma Pure Inc.), which formed phosphoric acid when they were exposed to ambient RH levels and subsequently removed NH_3 from the ambient air (Nowak et al., 2006, 2007). In either mode, the sample air passed through the common port of the 3-way valve and through 20 cm of FEP tubing into the CIMS inlet (1/4 inch ID). There was another PFA tee between the scrubber housing and the 3-way valve with a pump attached to constantly suck out 100 to 200 sccm during the ambient measurement mode. The flow through the inlet was as high as 15 slpm; the typical residence time in ambient and background mode was 68 ms. Of this total flow, 5.2 slpm flew into the CIMS flow reactor, and the rest was exhausted via a mass flow controller through a diaphragm pump. During the fall season, all tubing as well as all tees and valves were maintained at a constant temperature of about 35 °C. This was done by wrapping the tubing and valves in aluminum foil that was heated using heating tape. Keeping at a constant temperature for the inlet was important for preventing temperature fluctuations in the inlet tubing and reducing the uncertainties in background signals (Sect. 3.2).

The sensitivity of the CIMS instrument was measured by the use of standard addition calibrations using a known amount of NH_3 gases. Calibration was made with the least perturbation of flow using a solenoid valve (Fig. 1), similarly to (Nowak et al., 2006, 2007). The standard gas supplied from a source cylinder (Linde, mixing ratio 4.5 ppmv, ±5%) was added to the system with the flow between 1–10 sccm via a mass flow controller (MKS, ±0.6%), which was regularly calibrated with a DryCal (Bios). The NH_3 gases were added to a PFA tee along with a flow of N_2 gas from a liquid Dewar (Linde). The extra N_2 gases were added so that the total flow is high enough to produce a short residence time (<1 s) of the NH_3/N_2 mixture in the tee. This mixture was then introduced into another PFA tee with one port connected to the solenoid valve and another port attached to a third PFA tee on the inlet tubing (Fig. 1). When performing calibration measurement, the solenoid valve was closed and this gases entered into the inlet tubing. The resulting change in the signal was used to calculate the instrument sensitivity, which was usually given in the unit of Hz/pptv for certain amount of total reagent ions, for example, about 20 Hz/pptv for over 1 MHz of reagent ion signals. During the ambient measurement mode, however, the solenoid valve was open and the NH_3/N_2 gas mixture was removed through the solenoid valve (50–200 sccm), to minimize the flow and pressure changes in calibration system.

2.3 Flow tube for chemical ionization

Ion molecule reaction cell of the CIMS was maintained at a low pressure between 20–25 torr (1 torr=133.3 Pascal). The total flow through the reactor varied from 6.7–7.7 slpm and consisted of a constant flow of 5.2 slpm of ambient air through a 0.8 mm hole in an Al sampling cone and 1.5–2.5 slpm of ion source flow perpendicular to the ambient flow. The ion flow consisted mostly of N_2 with a small percentage (2–3%) of ethanol provided by flowing 50 sccm of N_2 through a small glass bottle containing 95% ethanol at room temperature. The N_2 flow through the ion source and N_2 flow through the bottle containing ethanol were regulated with mass flow controllers (MKS). The estimated reaction time in the flow reactor was 40 s.

The ion source flow was passed over a ^{210}Po radioactive source emitting α particles that led to the production of protonated ethanol ions and cluster ions $[(C_2H_5OH)_nH^+]$ in which n=1,2,3, etc. (Nowak et al., 2006). These ions reacted with NH_3 under the following pathway (Nowak et al., 2006):

$$[(C_2H_5OH)_nH^+ + NH_3 \rightarrow NH_3(C_2H_5OH)_{n-y}H^+ + y(C_2H_5OH) \qquad \text{(R1)}$$

where y is an integer less than or equal to n. A typical mass spectrum taken from the ambient air is shown in Fig. 2. The main ethanol cluster ions produced were monomer, $[(C_2H_5OH)H^+$; 47 amu], dimer, $[(C_2H_5OH)_2H^+$; 93 amu], and trimer, $[(C_2H_5OH)_3H^+$; 139 amu]. Larger sizes of weakly bound water clusters $[H_2O(C_2H_5OH)_nH^+]$ could also from in the reaction region, but use of a collision dissociation chamber (CDC) destroyed these weakly bounded larger ion clusters (Nowak et al., 2002, 2006). As a result, the main product ions were NH_4^+ (18 amu), $NH_3(C_2H_5OH)H^+$ (64 amu) and $NH_3(C_2H_5OH)_2H^+$(110 amu) (Fig. 2). The largest product ion peak was at 64 amu, so we used this peak to determine NH_3 mixing ratios. For NH_3 mixing ratio calculations, the sum of all the major reagent ions (47, 93, and 139 amu) was used to normalize the ambient signal to correct for the slight variation in pressure in the flow tube reactor which would cause fluctuations in these ion signals. Sensitivity was determined by taking the difference in the normalized signal between calibration and ambient mode and by dividing by the amount of the added calibration gases and then multiplying by the total reagent ion signal. For the same day, sensitivity values are nearly constant, although there were day to day variations. We used the average value of sensitivity of each day to calculate ambient NH_3 mixing ratios.

3 Evaluation of NH_3-CIMS

3.1 Time response

Data from our CIMS instrument was collected at a time resolution of 1 s. This data was further used to determine the time response for the instrument. Measuring the signal decay from removal of a standard addition calibration, the data can be fit by an exponential function (Ryerson et al., 2000) and the time response can be determined from the $1/e^2$ decay mark. For example, for one of the decays shown in Fig. 3, the fit was:

$$\%\text{Steady State } [NH_3] = 3 + 14e^{-0.018t} + 88e^{-0.524t} \quad (1)$$

The preexponential terms represent percentages of the steady state calibration level and t is the time in seconds after removal of calibration gases. For most decays, the time for the signal to reach $1/e^2$ (13.5%) of the initial signal (before calibration termination) was found to be less than 30 s.

We have also tried adding the calibration gases in different manners, for example, just 1 sccm of calibration gas flow, 50 sccm of N_2 and 1 sccm of calibration gas flow, 100 sccm of N_2 and 1 sccm of calibration gas flow. As shown in Fig. 4a, the signal rise was much faster with the additional N_2 flow. Without N_2, it took 5 min to reach steady state, whereas with the additional flow of 100 sccm of N_2 the signal reached steady state in less than a minute. Also shown in Fig. 4a is the instrument response to calibration gases with 400 pptv NH_3 added to our flow tube. This response is approximately what should be expected based on the calibration measurements with 800 pptv NH_3.

3.2 Background and its uncertainty

During the fall 2009 season, background measurements were performed for 5 min every 30 min period (Fig. 4b). The instrument background was usually below 1 ppbv and was as low as 300 pptv. This background signals varied with ambient NH_3 measurements, indicating that the majority of the background source was the desorption of NH_3 from inlet surfaces and/or in the ion-molecule reaction region (Nowak et al., 2006), rather than those possible NH_3 impurities coming from the standard N_2 and ethanol gases.

The background mixing ratio was determined in two ways. In the first method, the average NH_3 mixing ratio during the background mode was used (Background 1). The second method used the minimum NH_3 mixing ratio during the period (Background 2). If the uncertainty within the same calibration period is low enough, the two methods should give similar results. A comparison of the two methods is shown in Fig. 5a. The fall and the winter data show the best correlation between the two methods. For the spring data, there was a slight difference between the two methods (13%). This difference was due to a longer time response for background measurements to reach steady state during the spring measurements. We used the average background values (Background 1) in this study. No clear RH and temperature dependence was observed for background signals.

Uncertainty in background measurements includes the standard deviation (1σ) for each background measurement mode and the variation between two consecutive background measurements (Nowak et al., 2007). For the winter and fall measurements, both these uncertainties together were very low, less than 30 pptv. For the spring, the 1σ deviation was about 100 pptv between consecutive backgrounds, while the average difference was 200 pptv. As the fall measurements were made with a heated inlet system, these results show it is necessary to heat the system at constant temperature for NH_3 measurements.

3.3 Sensitivity and its uncertainty

Calibrations were usually made over 5 min every 3 h (Fig. 4b). The instrument sensitivity was estimated with two methods. Sensitivity 1 was taken from the difference between the initial point and final point from the calibration period and by dividing this difference by the calibration gas mixing ratio. Sensitivity 2 was taken by fitting the signal rise during the calibration period and using the maximum value from the fitting, as shown green symbol in Fig. 5b. Both sensitivities were between 4–25 Hz/pptv, and these two methods often had similar values (Fig. 5c), signifying that the steady state signal was readily achieved during 5 min of calibration. For the data that did not fit, Sensitivity 2 was about 1.1 times of Sensitivity 1. For calculations of NH_3 mixing ratio, Sensitivity 2 was used. No clear RH and temperature dependence was observed for sensitivity.

The uncertainties associated with sensitivity measurements came from the flow controllers and NH_3 source gases used to perform a calibration measurement, as well as the variability in calibration signals from a series of measurements. The uncertainty from the flow controllers was very low (<1%) and the NH_3 source cylinder had about a 5% uncertainty. The most uncertainty was caused by the variability of the calibration signals. This variability varied by season and was found highest for the fall (30%). These together led to the overall uncertainty 30%.

4 Ambient measurements

Figure 6 shows ambient measurements taken during a 9 day period for fall 2009. Included are the raw mass spectra signals for 64 amu (product ion) and 93 amu (reagent ion), Sensitivity 2, background NH_3 (Background 1), and ambient NH_3 mixing ratios. The reagent ion signal ranged between 600 000 and 700 000 Hz, depending on the flow tube pressure. The product ion signal ranged from 7000 to 30 000 Hz, and varied with the same trend as the reagent signal. The background and ambient NH_3 during this time period was 300–800 pptv and 50–400 pptv, respectively. For our CIMS, the background NH_3 was also often higher than the ambient NH_3 and varied with the ambient NH_3. Nowak et al. have shown that CIMS NH_3 background values can be lower or higher under different atmospheric conditions and locations (Nowak et al., 2007).

The ambient measurements taken for the fall, spring and winter of 2009 are shown in Fig. 7. For all three seasons, it was clear that the NH_3 mixing ratio present in Kent was always below 1 ppbv. Overall the median NH_3 (with 1σ deviation) for each season was 60±75 pptv for winter, 200±120 pptv for spring, and 150±80 pptv for fall. The maximum NH_3 for each season was 250 pptv for winter, 430 pptv for spring and 300 pptv for fall. There was also positive dependence of ambient NH_3 on temperature for all seasons, especially for the winter and spring. The spring had the highest temperatures, which is a possible explanation for the slightly higher NH_3 mixing ratios during this season. However, RH dependence for NH_3 was rather unclear, for example, positive for the winter and negative for the spring and fall. There was no distinctive diurnal variation for the ambient NH_3, even though there were substantial hourly variations.

We have performed NOAA trajectory (Draxler and Rolph, 2010; Rolph, 2010) calculations and also derived wind direction and speed information from Weather Underground (www.wunderground.com), to see how air mass history affected local NH_3 mixing ratio. These analysis show that air masses often originated from northwest in spring and fall and from west/northwest in winter. From EPA ammonia emission data (http://www.epa.gov/cgi-bin/broker?_service=airdata&_program=progs.webprogs.emisdist.scl&_debug=2&geotype=st&geocode=OH&geoname=Ohio&empol=NH3&emyear=2002&emtype=&emtier=&emval=a&mapsize=zsc&reqtype=viewmap) where the most current data posted are only for 2002, one would expect that airmass traveling from NW would contain higher concentrations. This could also explain why NH_3 mixing ratio was higher in spring and fall, but more recent emission data are needed to address the transport effects on the NH_3 mixing ratio.

5 Discussion

There have been three different CIMS instruments for NH_3 detection found in literature (Nowak et al., 2006; Norman et al., 2007; Nowak et al., 2007). Table 1 summarizes these previous NH_3-CIMS instruments, including inlet and CIMS parameters. The reagent ions used were protonated ethanol ($CH_3CH_2OH\text{-}H^+$), protonated acetone ($CH_3CO\ CH_3\text{-}H^+$), and positive oxygen (O_2^+). The main difference between them was that in the first two cases, the product ions consisted of NH_4^+ and protonated cluster ions ($NH_3(C_2H_5OH)_nH^+$), whereas the third method employed electron transfer to produce NH_3^+. One reason for choosing the O_2^+ method over the NH_4^+/proton cluster method was that the use of O_2 can possibly limit the amount of background NH_3 produced in the ion source .(Norman et al., 2007). For the NH_4^+/proton cluster methods, the residence times were usually in the 20–160 ms, whereas for the O_2^+ method the time was 0.1–0.15 ms to minimize secondary reactions with NH_3^+.(Norman et al., 2007). The sensitivity and background were also different for the two techniques. For the NH_4^+/proton cluster method, the sensitivity (1–40 Hz/pptv) and the background (up to 2 ppbv) both were higher than those in the electron transfer scheme (0.04 Hz/pptv sensitivity and up to 0.47 ppbv background). While protonated ethanol ions ($CH_3CH_2OH\text{-}H^+$) have been shown to give higher sensitivity, protonated acetone ions ($CH_3COCH_3\text{-}H^+$) can be less prone to NH_3 contamination (Huey, 2007; Nowak et al., 2007). For the present study, using protonated ethanol has produced a moderate sensitivity as well as relatively lower background. Most of these CIMS utilized a low pressure (<25 torr) in the reaction region, although there are advantages with atmospheric pressure chemical ionization, such as enhanced CIMS sensitivity (Huey, 2007).

For the NH_3 sampling inlet, the most important features are its configuration, the residence time in the inlet, and maintenance of the inlet at a heated constant temperature. Having a straight flow path from the inlet tip to the CIMs can reduce possible losses from having curves in the tubing. Our inlet configuration was not perfectly straight (due to the commercial 3-way valve used in this study) (Fig. 1), and we are currently building a custom made 3-way valve using PFA teflon based on (Nowak et al., 2006) to allow ambient air to flow straight through to CIMS. It is also important to keep the inlet as short as possible and to have a high enough flow so that the residence time inside the inlet will be minimized. This would allow a short response time from the inlet to the CIMS so that rapid changes in ambient NH_3 can be measured at real-time. Maintenance of a constant temperature is also important for the inlet as this prevents temperature fluctuations, which may lead to adsorption/desorption of NH_3 on the inlet walls (Nowak et al., 2007).

Our measurements made in Kent show that the NH_3 mixing ratios were lowest in the winter (60±75 pptv) and higher in the spring (200±120 pptv) and fall (150±80 pptv) (Fig. 7). In comparison, NH_3 mixing ratios in the remote marine atmosphere were 86 pptv on average (Schlesinger and Hartley, 1992) and as low as 20 pptv in some remote areas (Dentener and Crutzen, 1994). On the other hand, polluted areas have shown mixing ratios as high as 30 ppbv (Dentener and Crutzen, 1994) and mixing ratio up to 430 ppb have been seen in strong point source locations (Schlesinger and Hartley, 1992). For example, in New York City, an average NH_3 mixing ratio of 800 pptv was measured during one winter month (Li et al., 2006). Emissions made in the Van Nuys tunnel in L.A., California also showed background NH_3 mixing ratio of 3 ppbv and mixing ratios in the tunnel of 50 ppbv (Fraser and Cass, 1998). A similar study in San Francisco showed mixing ratios ranging from 21–53 ppbv at the tunnel entrance and 333–403 ppbv at the tunnel exit on a summer evening (Kean et al., 2000). Another study of auto emissions in Switzerland showed tunnel mixing ratios of 200–400 ppbv (Moeckli et al., 2004). NH_3 mixing ratios of 20–70 ppbv have been reported from smoke plumes (Yokelson et al., 1999; Goode et al., 2000) as well as mixing ratio as high as 100–200 ppbv in plumes from biomass burning (Hurst et al., 1994; Yokelson et al., 2003; Li et al., 2006). These comparisons suggest that Kent has much less emissions of NH_3 year around, mainly because of low level of automobile emissions.

6 Conclusions

We have used a CIMS to measure ambient NH_3, using protonated ethanol ions as reagent. The sensitivity for the CIMS ranged from 4–25 Hz/pptv with a maximum uncertainty of 30% for over 1 MHz of reagent ion signal. The time response determined from the decay of the calibration signal was less than 30 s. The background NH_3 was in the range 0.3–1 ppbv with an uncertainty of 30 pptv under the optimized experimental condition. The detection limit of the instrument was estimated to be about 60 pptv.

This newly developed NH_3-CIMS has been used in ambient observations in Kent, Ohio during several weeks through three seasons. NH_3 mixing ratios were higher during the spring (200±120 pptv) than in the winter (60±75 pptv) and fall (150±80 pptv). Our observations show that the NH_3 in this region was always at the sub-ppbv level. NH_3 has been used to theoretically explain new particle formation in Eastern US (Stanier et al., 2004; Gaydos et al., 2005; Jung et al., 2008). But the current aerosol nucleation theories use the NH_3 mixing ratio only from 0–100 pptv in their parameterizations (Merikanto et al., 2007). Our atmospheric observations, together with other observations discussed in this study, suggest that these nucleation theories should be revised to include a larger range of NH_3 in their parameterizations to represent atmospheric conditions.

There have been only three CIMS instruments used for NH_3. While our CIMS has the sensitivity sufficient for ambient measurements, there is a large room to improve our CIMS, especially in order to reduce instrument background signals and time response so that, for example, we can indentify NH_3 sources and investigate the NH_3 effects on new particle formation at real time. One of these improvements is to build a custom made 3-way valve in PFA Teflon, in which ambient sampling could be performed in a straight through manner to reduce any losses that can occur due to curves in the tubing. We also want to reduce the tubing length in the inlet system further to reduce the residence time. We will also improve our heating system so the entire inlet system will be heated uniformly to reduce background signals and the uncertainties resulted from background signals.

Acknowledgements. We gratefully acknowledge funding support from NOAA (NA08OAR4310537), NSF (CAREER ATM-0645567; ATM-0904144) and Ohio Board Regents. We also thank Greg Huey, David Tanner, John Nowak, and Bob Yokelson for useful discussions and suggestions.

References

Ball, S. M., Hanson, D. R., Eisele, F. L., and McMurry, P. H.: Laboratory studies of particle nucleation: Initial results for H_2SO_4, H_2O, and NH_3 vapors, J. Geophys. Res., 104, 23709–23718, 1999.

Benson, D. R., Erupe, M. E., and Lee, S.-H.: Laboratory-measured H_2SO_4-H_2O-NH_3 ternary homogenous nucleation rates: Initial observations, Geophys. Res. Lett., 36, L15818, doi:10.1029/2009GL038728, 2009.

Benson, D. R., Young, L. H., Kameel, R., and Lee, S.-H.: Laboratory-Measured Sulfuric Acid and Water Homogeneous Nucleation Rates from the SO2+OH Reaction, Geophys. Res. Lett., 35, L11801, doi:11810.11029/12008GL033387, 2008.

Dentener, F. J. and Crutzen, F.: A three-dimensional model of the global ammonia cycle J. Atmos. Chem., 19, 331–369, 1994.

Draxler, R. R. and Rolph, G. D.: HYSPLIT (HYbrid Single-Particle Lagrangian Integrated Trajectory) Model access via NOAA ARL READY Website (http://ready.arl.noaa.gov/HYSPLIT.php), NOAA Air Resources Laboratory, Silver Spring, MD, 2010.

Eisele, F. L. and Tanner, D. J.: Measurements of gas phase concentrations of H_2SO_4 and methane sulfonic acid and estimates of H_2SO_4 production and loss in the atmosphere J. Geophys. Res., 98, 9001–9010, 1993.

Fehsenfeld, F. C., Huey, L. G., Leibrock, E., Dissley, R., Williams, E., Ryerson, T. B., Norton, R., Sueper, D. T., and Hartsell, B.: Results from an informal intercomparison of ammonia measurement techniques J. Geophys. Res., 107, 4812–4819, doi:4810.1029/2001JD001327, 2002.

Ferm, M., Areskoug, H., Hanssen, J.-E., Hilbert, G., and Lattila, H.: Field Intercomparison of Measurement Techniques for Total NH_4^+ and Total NO_3^- in Ambient Air, Atmos. Environ., 22(10), 2275–2281, 1988.

Fraser, M. P. and Cass, G. R.: Detection of excess ammonia emissions from in-use vehicles and the implications for fine particle control Environ. Sci. Technol., 32, 1053–1057, 1998.

Gaydos, T. M., Stainer, C. O., and Pandis, S. N.: Modeling of in situ ultrafine atmospheric particle formation in the eastern United States, J. Geophys. Res., 110, D07S12, doi:10.1029/2004JD004683, 2005.

Gilliland, A. B., Dennis, R. L., Roselle, S. J., and Pierce, T. E.: Seasonal NH_3 emission estimates for the eastern United States based on ammonium wet concentrations and an inverse modeling method, J. Geophys. Res., 108, 4477, doi:4410.1029/2002JD003063, 2003.

Goode, J. G., Yokelson, R. J., Ward, D. E., Susott, R. A., Babbit, R. E., Davies, M. A., and Hao, W. M.: Measurements of excess O_3, CO_2, CH_4, C_2H_4, HCN, NO, NH_3, HCOOH, CH_3COOH, HCHO, and CH_3H in 1997 Alaskan biomass burning plumes by airborne Fourier transform infrared spectroscopy, J. Geophys. Res., 105, 22417–22166, 2000.

Herndon, S. C., Jayne, J. T., Zahniser, M. S., Worsnop, D. R., Knighton, B., Alwine, E., Lamb, B. K., Zavala, M., Nelson, D. D., McManus, J. B., Shorter, J. H., Canagaratna, M. R., Onasch, T. B., and Kolb, C. E.: Charecterization of urban pollutant emission fluxes and ambient concentration distributions using a mobile laboratory with rapid response instrumentation, Faraday Disc., 130, 327–339, 2005.

Huai, T., Durbin, T. D., Miller, J. W., Pisano, J. T., Saucer, C. G., Rhee, S. H., and Norbeck, J. M.: Investigation of NH_3 emissions from new technology vehicles as a function of vehicles as a function of vehicle operating conditions Environ. Sci. Technol., 37, 4841–4847, 2003.

Huey, L. G.: Measurement of trace atmospheric species by chemical ionization mass spectrometry: Speciation of reactive nitrogen and recent developments, Mass Spectrom. Rev., 26, 166–184, 2007.

Hurst, D. F., Griffith, D. W. T., Carras, J. N., Williams, D. J., and Freser, P. J.: Measurements of trace gases emitted by Australian savanna fires during the 1990 dry season, J. Atmos. Chem., 18, 33–56, 1994.

Jung, J. G., Pandis, S. N., and Adams, P. J.: Evaluation of Nucleation Theories in a Sulfur-Rich Environment, Aerosol Sci. Technol., 42, 495–504, 2008.

Kean, A. J., Harley, R. A., Littlejohn, D., and Kendall, G. R.: On-road measurement of ammonia and other motor vehicle exhaust emissions Environ. Sci. Technol., 34, 3535–3539, 2000.

Langford, A. O., Golden, P. D., and Fehsenfeld, F. C.: A molybdenum oxide annular denuder system for gas-phase ambient ammonia measurement J. Atmos. Chem., 8, 359–376, 1989.

Title Page
Abstract Introduction
Conclusions References
Tables Figures
◀◀ ▶▶
◀ ▶
Back Close
Full Screen / Esc
Printer-friendly Version
Interactive Discussion

Lebel, P. J., Hoell, J. M., Levine, J. S., and Vay, S. S.: Aircraft measurements of ammonia and nitric acid in the lower troposphere, Geophys. Res. Lett., 12, 401–404, 1985.

Li, Y., Schwab, J. J., and Demerijian, K. L.: Measurements of ambient ammonia using a tunable diode laser absorption spectrometer: Characteristics of ambient ammonia emissions in an urban area of New York City, J. Geophys. Res., 111, D10S02, doi:10.1029/2005JD006275, 2006.

Lucas, D. D. and Akimoto, H.: Evaluating aerosol nucleation parameterization in a global atmospheric model, Geophys. Res. Lett., 33, L10808, doi:10810.11029/12006GL025672, 2006.

McMurry, P. H., Fink, M., Sakuri, H., Stolzenburg, M., Mauldin III, R. L., Smith, J., Eisele, F. L. M., K., Sjostedt, S., Tanner, D., Huey, L. G., Nowak, J. B., Edgerton, E., and Voisin, D.: A criterion for new partricle formation in the sulfur-rich Atlanta atmosphere, J. Geophys. Res., 110, D22S02, doi:10.1029/2005JD005901, 2005.

Merikanto, J., Napari, I., Vehkamäki, H., Anttila, T., and Kulmala, M.: New parameterization of sulfuric acid-ammonia-water ternary nucleation rates at tropospheric conditions, J. Geophys. Res., 112, D15207, doi:15210.11029/12006JD007977, 2007.

Moeckli, M., Fierz, M., and Sigritism, M. W.: Emissions factors for ethane and ammonia from a tunnel study with a photoacoustic trace gas detection system Environ. Sci. Technol., 30, 2864–2867, 2004.

Neuman, J. A., Huey, L. G., Dissly, R. W., Fehsenfeld, F. C., Flocke, F., Holecek, J. C., Holloway, J. S., Hubler, G., Jakoubek, R., Nicks Jr., D. K., Parrish, D. D., Ryerson, T. B., Sueper, D. T., and Weinheimer, A. J.: Fast-response airborne in situ measurements HNO_3 during the Texas 2000 Air Quality Study, J. Geophys. Res., 107(D20), 4436, doi:10.1029/2001JD001437, 2002.

Norman, M., Hansel, A., and Wisthaler, A.: O_2^+ as reagent ion in the PTR-MS instrument: Detection of gas-phase ammonia, Int. J. Mass Spectrom., 265, 382–387, 2007.

Nowak, J. B., Huey, L. G., Eisele, F. L., Tanner, D., Mauldin III, R. L., Cantrell, C. A., Kosciuch, E., and Davis, D.: Chemical ionization mass spectrometry technique for the detection of dimethylsulfoxide and ammonia, J. Geophys. Res., 107(D18), 4363, doi:4310.1029/2001JD001058, 2002.

Nowak, J. B., Huey, L. G., Russell, A. G., Tian, D., Neuman, J. A., Orsini, D., Sjostedt, S. J., Sullivan, A. P., Tanner, D. J., Weber, R. J., Nenes, A., Edgerton, E., and Fehsenfeld, F. C.: Analysis of urban gas phase ammonia measurements from the 2002 Atlanta Aerosol Nucleation and Real-Time Characterization Experiment (ANARChE), J. Geophys. Res., 111, D17308, doi:17310.11029/12006JD007113, 2006.

Nowak, J. B., Newman, J. A., Kozai, K., Huey, L. G., Tanner, D., Holloway, J. S., Ryerson, T. B., Frost, G. L., McKeen, S. A., and Fehsenfeld, F. C.: A chemical ionization mass spectrometry technique for airborne measurements of ammonia, J. Geophys. Res., 112, D10S02, doi:10.1029/2006JD007589, 2007.

Quinn, P. K. and Bates, T. S.: Collection efficiences of a tandem sampling system for atmospheric aerosol particles and gaseous ammonia and sulfur dioxide, Environ. Sci. Technol., 23, 736–739, 1989.

Rolph, G.D.: Real-time Environmental Applications and Display sYstem (READY) Website (http://ready.arl.noaa.gov), NOAA Air Resources Laboratory, Silver Spring, MD, 2010.

Ryerson, T. B., Williams, E. J., and Fehsenfeld, F. C.: An efficient photolysis system for fast response NO_2 measurements, J. Geophys. Res., 105(D21), 26447–26461, 2000.

Schlesinger, W. H. and Hartley, A. E.: A global budget for atmospheric NH_3, Biogeochemistry, 15, 191–211, 1992.

Schwab, J. J., Li, Y., Bae, M.-S., Demerjian, K. L., Hou, J., Zhou, X., Jensen, B., and Pryor, S. C.: A Laboratory Intercomparison of Real-Time Gaseous Ammoni Measurement Methods, Environ. Sci. Technol., 41(24), 8412–8419, 2007.

Slusher, D. I., Huey, L. G., Tanner, D. J., Flocke, F. M., and Roberts, J. M.: A thermal dissociation-chemical ionization mass spectrometry (TD-CIMS) technique for the simultaneous measurement of peroxyacyl nitrates and dinitrogen pentoxide, J. Geophys. Res., 109, D19315, doi:10.1029/2004JD004670, 2004.

Smith, J. N., Moore, K., Eisele, F. L., Voisin, D., Ghimire, A. K., Sakuri, H., and McMurry, P. H.: Chemical composition of atmospheric nanoparticles during nucleation in Atlanta, J. Geophys. Res., 110, D22S03, doi:10.1029/2005JD005912, 2005.

Stanier, C. O., Kylstov, A. Y., and Pandis, S. N.: Nucleation events during the Pittsburgh air quality study: Description and relation to key meteorological, gas phase, and aerosol parameters, Aerosol Sci. Tech, 38, 253–264, 2004.

van Dijk, C. A., Sandholm, S. T., Davis, D. D., and Bradshaw, J. D.: NH($b^1\Sigma^+$) deactivation/reaction rate constants for the collisional gases $H_{2,}$$CH_4$, C_2H_6, Ar, N_2, O_2, H_2O and CO_2, J. Phys. Chem.-US, 93, 6363–6767, 1989.

Weber, R. J., Marti, J. J., McMurry, P. H., Mauldin III, R. L., Tanner, D., Eisele, F. L., Brechtel, F., Kreidenweis, S. M., Kok, G., Schillawski, R. D., and Baumgardner, D.: A study of new particle formation and growth involving biogenic and trace gas species measured during ACE 1, J. Geophys. Res., 103, 16385–16396, 1998.

Yokelson, R. J., Bertschi, I. T., Christian, T. J., Hobbs, P. V., Ward, D. E., and Hao, W. M.: Trace gas measurements in nascent, aged, and cloud processed smoke from African savanna fires by airborne Fourier transform infrared spectroscopy (AFTIR), J. Geophys. Res., 108(D13), 8478, doi:8410.1029/2002JD002322, 2003.

Yokelson, R. J., Christian, T. J., Bertschi, I. T., and Hao, W. M.: Evaluation of adsorption effects on measurements of ammonia, acetic acid, and methanol, J. Geophys. Res., 108(D20), 4649, doi:10.1029/2003JD003549, 2003b.

Yokelson, R. J., Goode, J. G., Ward, D. E., Susott, R. A., Babbitt, R. E., Wade, D. D., Bertschi, I., Griffith, D. W. T., and Hao, W. M.: Emissions of formaldehyde, acetic acid, methanol, and other trace gases from biomass fires in North Carolina measured by airborne Fourier transform infrared spectroscopy, J. Geophys. Res., 104, 30109–30126, 1999.

Young, L. H., Benson, D. R., Kameel, F. R., Pierce, J. R., Junninen, H., Kulmala, M., and Lee, S.-H.: Laboratory studies of H_2SO_4/H_2O binary homogeneous nucleation from the SO_2+OH reaction: evaluation of the experimental setup and preliminary results, Atmos. Chem. Phys., 8, 4997–5016, 2008, http://www.atmos-chem-phys.net/8/4997/2008/.

Title Page
Abstract
Introduction
Conclusions
References
Tables
Figures
◀
▶
Back
Close
Full Screen / Esc
Printer-friendly Version
Interactive Discussion

Table 1. A summary of NH_3-CIMS instruments found in the literature, with regard to sampling inlet and CIMS detection conditions. Included here are the configuration of 3-way valve used to switch between the ambient and calibration mode, the temperature, flow rate, total length and inner diameter of the sampling inlet, the residence time for ambient measurements through the inlet, the pressure and residence time in the CIMS flow tube reactor, the ion reagent used to ionize NH_3 molecules, the sensitivity, background, and time response of the CIMS instrument.

Reference	3-way valve Configuration[f]	Inlet Temperature (°C)	Inlet Flow Rate (slpm)	Inlet Length (cm)	Inlet ID (cm)	Inlet Residence Time (ms)[g]
Nowak et al. (2006)[a]	Straight	50	4	45	0.4, 0.64	200
Nowak et al. (2006)[b]	Straight	40	13.6	40	0.65	50
Nowak et al. (2007)[c]	Straight	30	8	55	0.4, 0.8	190
Norman et al. (2007)[d]	NA	NA	15	1700	1.27	NA
This study[e]	Bent	35[j]	5.2–15	100[k]	0.4	68[i]

[a] This early version of NOAA-CIMS was used in Atlanta, GA during August 2002 for the Aerosol Nucleation and Real-Time Characterization Experiment (ANARChE). Measurements were performed at an urban site 2 meters above the ground level.

[b] The GaTech-CIMS was also used for the ANARChE and intercomparison with the early version of NOAA-CIMS was made.

[c] This upgraded NOAA-CIMS for aircraft measurements were used in the New England Air Quality Study–Intercontinental Transport and Chemical Transformation (NEAQS-ITCT) mission.

[d] The CIMS instrument was used at 1.2 m above a grass field treated with fertilizer located in Oensingen, Switzerland.

[e] The KSU-CIMS was used at 15 m above the ground in Kent, Ohio (This study).

[f] Straight sampling occurred when the flow path from the tip of the inlet (where ambient air enters) through the 3-way valve and to the CIMS was all straight and no bending occurred. Bent sampling occurred when the ambient air entered the 3-way valve perpendicular to the flow that went into the CIMS as shown in Fig. 1.

[g] Residence time for ambient mode.

[h] This time was based on the flow rate through the CIMS flow tube and the dimensions (inner diameter and length).

[i] This time was based on the flow rate through the inlet and the inlet dimensions (inner diameter and length).

[j] Heating was only performed for the fall measurements, but not for spring or winter measurements.

[k] 100 cm was the total length when taking ambient measurements (including the depth of thewall, 50 cm).

Title Page
Abstract | Introduction
Conclusions | References
Tables | Figures
◀| |▶
◀ ▶
Back | Close
Full Screen / Esc
Printer-friendly Version
Interactive Discussion

Table 1. Continued.

Reference	CIMS Flow Tube Pressure (torr)	Reagent Ion	CIMS Flow Tube Residence Time (ms)[h]	Sensitivity (Hz/pptv)	Background (ppbv)	CIMS Time Response to Calibration Gases (s)
Nowak et al. (2006)[a]	Atmospheric Pressure	$CH_3CH_2OH\text{-}H^+$	–	1	0.1–1	10
Nowak et al. (2006)[b]	20	$CH_3CH_2OH\text{-}H^+$	20	40	1–2	45
Nowak et al. (2007)[c]	18–22	$CH_3COCH_3\text{-}H^+$	95–160	2.6–5	0.5–1.3	5
Norman et al. (2007)[d]	1.5	O_2^+	0.100–0.15	0.04	0.07–0.47	30
This Study[e]	20–25	$CH_3CH_2OH\text{-}H^+$	25–40	10–30	0.3–2	40

[a] This early version of NOAA-CIMS was used in Atlanta, GA during August 2002 for the Aerosol Nucleation and Real-Time Characterization Experiment (ANARChE). Measurements were performed at an urban site 2 meters above the ground level.

[b] The GaTech-CIMS was also used for the ANARChE and intercomparison with the early version of NOAA-CIMS was made.

[c] This upgraded NOAA-CIMS for aircraft measurements were used in the New England Air Quality Study–Intercontinental Transport and Chemical Transformation (NEAQS-ITCT) mission.

[d] The CIMS instrument was used at 1.2 m above a grass field treated with fertilizer located in Oensingen, Switzerland.

[e] The KSU-CIMS was used at 15 m above the ground in Kent, Ohio (This study).

[f] Straight sampling occurred when the flow path from the tip of the inlet (where ambient air enters) through the 3-way valve and to the CIMS was all straight and no bending occurred. Bent sampling occurred when the ambient air entered the 3-way valve perpendicular to the flow that went into the CIMS as shown in Fig. 1.

[g] Residence time for ambient mode.

[h] This time was based on the flow rate through the CIMS flow tube and the dimensions (inner diameter and length).

[i] This time was based on the flow rate through the inlet and the inlet dimensions (inner diameter and length).

[j] Heating was only performed for the fall measurements, but not for spring or winter measurements.

[k] 100 cm was the total length when taking ambient measurements (including the depth of thewall, 50 cm).

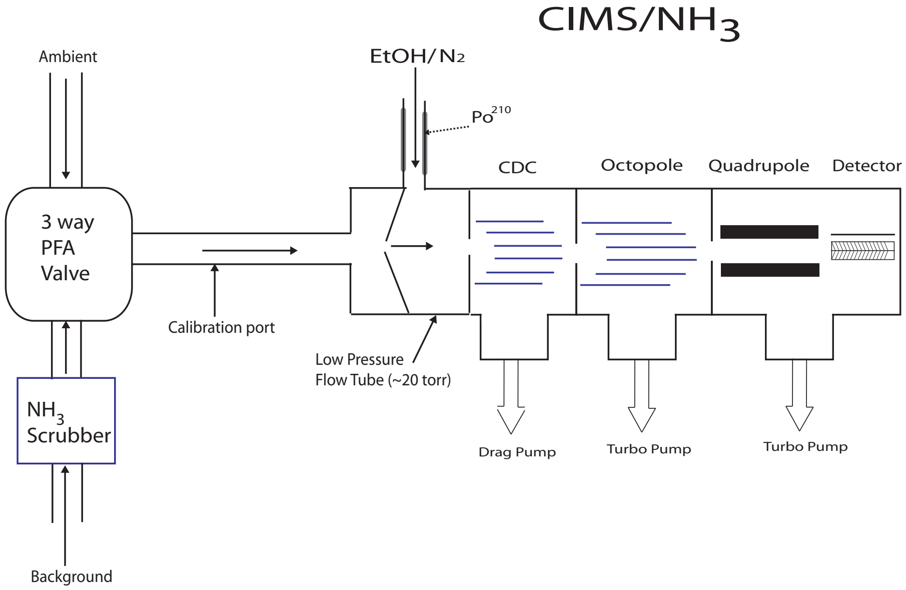

Fig. 1a. The NH_3-CIMS system consists of the following three parts: (i) a sampling inlet to perform ambient, background and calibration measurements, (ii) the CIMS flow reactor where ion-molecule reactions occur, and (iii) the vacuum regions of the mass spectrometer including a collision dissociation chamber (CDC), an octopole ion guide, a quadrupole mass filter and a channeltron detector.

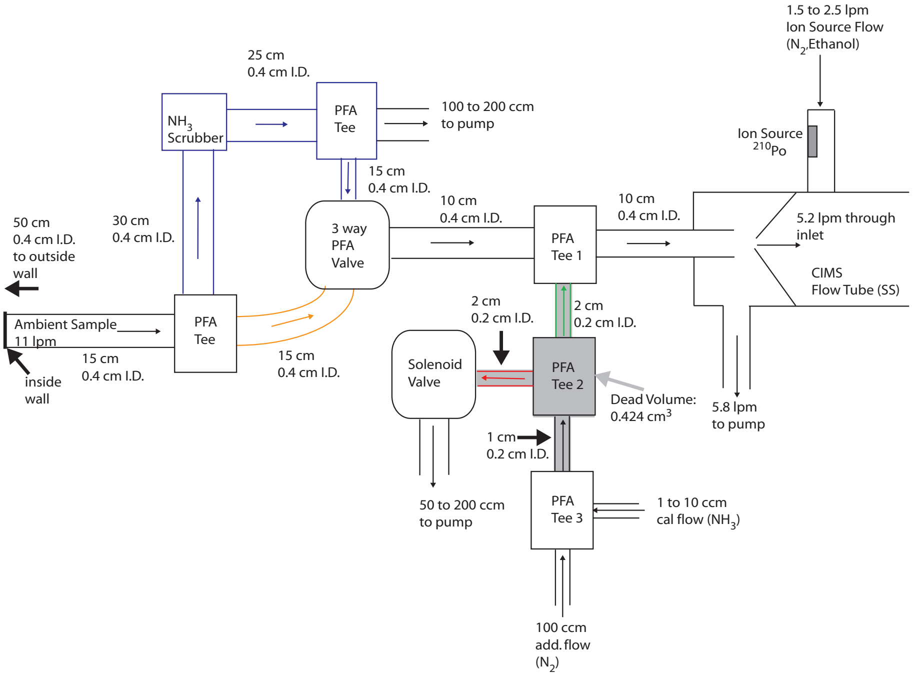

Fig. 1b. A schematic diagram of the inlet of KSU NH_3-CIMS used in the fall 2009 measurements. The air entered through an inlet port (11 slpm) and traveled through a PFA tee. The air flew either directly through a 3-way PFA valve (measurement mode) or through an NH_3 scrubber (background mode) and into the PFA valve. At the exit of the 3-way valve, the sample traveled into an inlet port on the CIMS. There was PFA Tee 1 located between the 3-way valve and the CIMS, to allow the calibration gases being introduced into the system. An additional flow (100 sccm) of N_2 gases were brought into the system through PFA Tee 3 to the system; this additional N_2 flow minimized the instrument residence time to the calibration gases. This time response was affected by both the flow rate of gases and the dead volume (shown in the grey shaded area; estimated to be 0.4 cm^3) in the tubing. When taking ambient or background measurements, the added calibration gases were removed by the suck back flow through PFA Tee 2 and a solenoid valve, to reduce perturbation of flow. The orange arrow and lines represent the flow for ambient measurements, the blue arrows and lines background measurements, the green arrow and lines the addition of calibration gases to the ambient sample, and the red arrow and lines the calibration gases being removed by the suck-back flow through the solenoid valve.

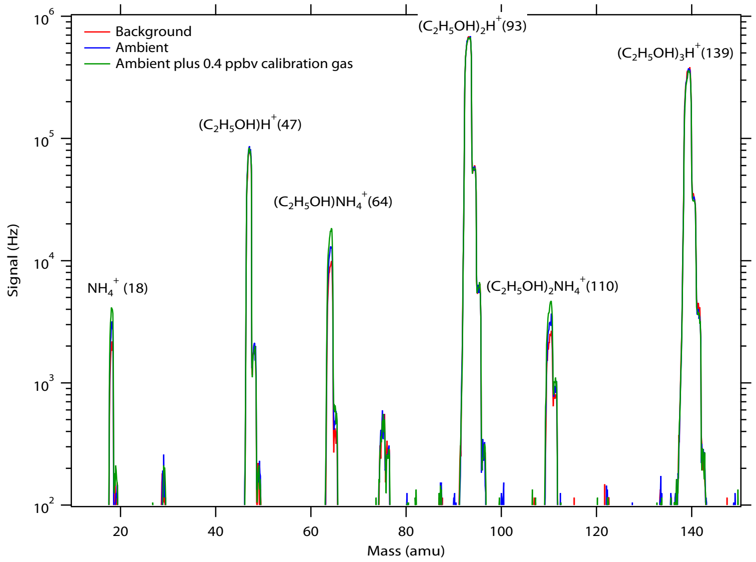

Fig. 2. Typical mass spectra taken for the background (red), ambient (blue), and ambient plus calibration mode (green). The main reagent ion signals were $(C_2H_5OH)H^+$ (47 amu), $(C_2H_5OH)_2H^+$ (93 amu), and $(C_2H_5OH)_3H^+$ (139 amu), and the main product ion signals were NH_4^+ (18 amu), $(C_2H_5OH)NH_4^+$ (64 amu) and $(C_2H_5OH)_3$ NH_4^+ (110 amu). To calculate NH_3 mixing ratios, we used the main product peak at 64 amu and normalized this with the sum of these three reagent ion signals. Larger clusters as well as weakly bound water clusters $[H_2O(C_2H_5OH)_nH^+]$ may also exist, but use of a collision dissociation chamber (CDC) effectively destroyed these weakly bounded larger ions; for example, ion intensities for peaks at >150 amu were insignificant.

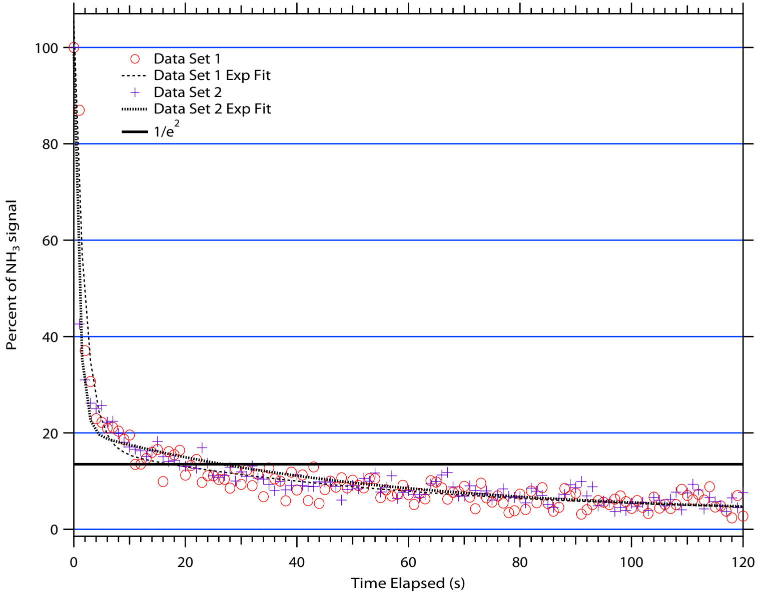

Fig. 3. Signal decays after removal of calibration. Two data sets were used to calculate the time response of the CIMS instrument. Data Set 1 was for a sensitivity of 24.5 Hz/pptv (maximum signal was 25 000 Hz) and Data Set 2 for a sensitivity of 36.8 Hz/pptv (maximum signal 35 000 Hz). The dotted/dashed lines represent double exponential fits for the data sets and the solid line $1/e^2$ decay.

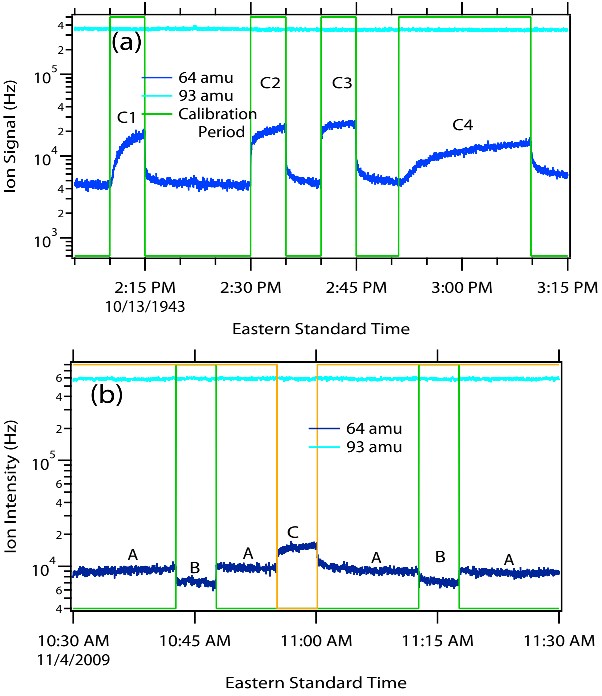

Fig. 4. (a) A mass spectra scanning sequence, showing four different calibration measurements with the major reagent [$(C_2H_5OH)_2H^+$, 93 amu] and product [$(C_2H_5OH)NH_4^+$, 64 amu] ion signals. C1 indicates the measurements made using only 0.8 ppbv NH_3 calibration gases without additional nitrogen flows, C2 using 0.8 ppbv NH_3 calibration gases and additional 50 sccm of N_2 flows, C3 using 0.8 ppbv NH_3 and additional 100 sccm of N_2, and C4 using 0.4 ppbv NH_3 and additional 100 sccm of N_2. **(b)** A typical sequence of mass spectra scan, including ambient (A), background (ambient air through NH_3 scrubber, B) and calibration mode (addition of calibration gases to sample line, C).

Title Page
Abstract
Introduction
Conclusions
References
Tables
Figures
◀
▶
Back
Close
Full Screen / Esc
Printer-friendly Version
Interactive Discussion

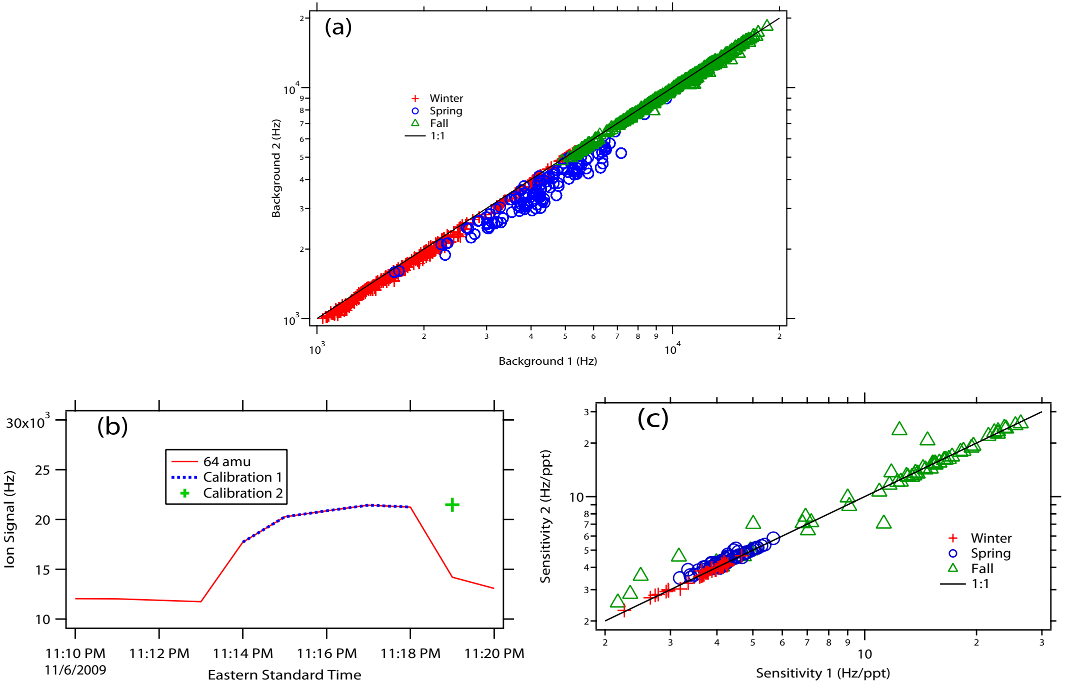

Fig. 5. (a) Correlation of two types of background signals, one taken from the average value of the product ion (64 amu) during a background period (Background 1) and the other taken from the minimum point of 64 amu during each background period (Background 2), for winter (red crosses), spring (blue open circles), and fall (green open triangles). The black solid line shows the 1:1 line between x and y axis, as opposed to the linear fitting of the data. Background 1 was used in the current study. **(b)** A typical calibration curve. Calibrations 1 (blue dotted) and 2 (green circle) were used in estimation of Sensitivities 1 and 2 (see text). **(c)** Correlation Sensitivities 1 and 2 during each calibration period, for winter (red crosses), spring (blue open circles), and fall (green open triangles). The black solid line shows the 1:1 line between x and y axis, rather than a linear fitting of the data.

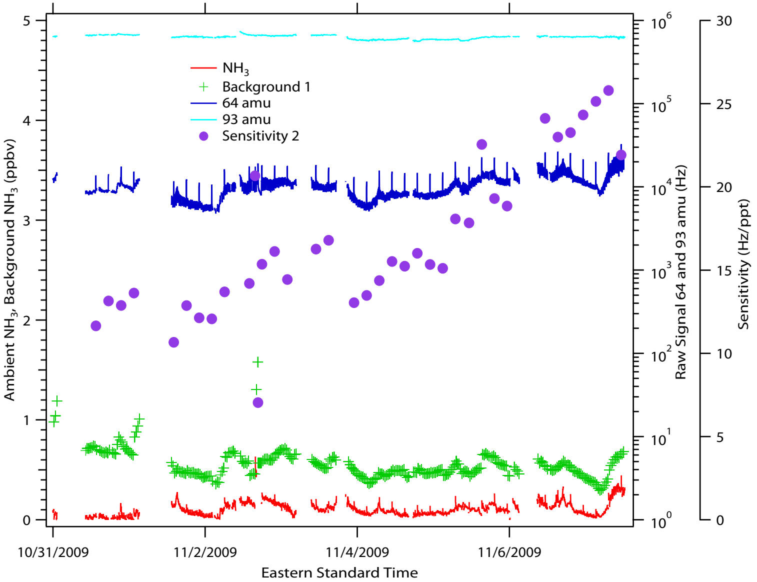

Fig. 6. Ambient measurements taken during the fall of 2009 over a 9 day span. Included are the main product (64 amu, blue solid line) and reagent ion mass signals (93 amu, cyan solid line), the CIMS background (Background 1, green crosses) and sensitivity (Sensitivity 2, purple closed circles), and the ambient NH$_3$ mixing ratios (red solid line).

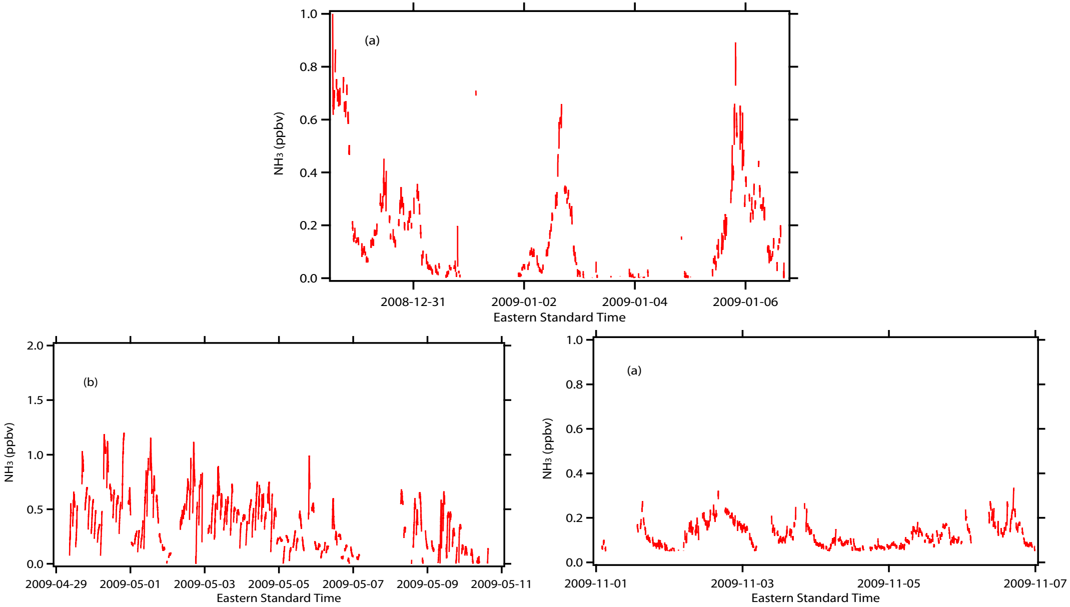

Fig. 7. Ambient NH_3 mixing ratios measured by CIMS in Kent, Ohio, during the winter over a 9 day span **(a)**, during the spring for 12 days **(b)**, and during the fall for 7 days **(c)**.